

Research Article

The Coupled Nonlinear Schrödinger Equations Describing Power and Phase for Modeling Phase-Sensitive Parametric Amplification in Silicon Waveguides

Xuefeng Li,¹ Zhaolu Wang,² and Hongjun Liu²

¹ School of Science, Xi'an University of Post & Telecommunications, Xi'an 710121, China

² Xi'an Institute of Optics and Precision Mechanics, Chinese Academy of Sciences, Xi'an 710119, China

Correspondence should be addressed to Xuefeng Li; lixpost@163.com

Received 16 June 2014; Revised 13 August 2014; Accepted 14 August 2014; Published 24 August 2014

Academic Editor: Ray K.L. Su

Copyright © 2014 Xuefeng Li et al. This is an open access article distributed under the Creative Commons Attribution License, which permits unrestricted use, distribution, and reproduction in any medium, provided the original work is properly cited.

The coupled nonlinear Schrödinger (NLS) equations describing power and phase of the optical waves are used to model phase-sensitive (PS) parametric amplification in a width-modulated silicon-on-insulator (SOI) channel waveguide. Through solving the coupled NLS equations by the split-step Fourier and Runge-Kutta integration methods, the numerical results show that the coupled NLS equations can perfectly describe and character the PS amplification process in silicon waveguides.

1. Introduction

Nowadays, silicon has emerged as a highly attractive material for nonlinear photonic integration [1]. Compared with highly nonlinear fiber, the SOI platform has inherent advantages due to the large values of Kerr parameter and Raman gain coefficient, the tight confinement of the optical mode, and the mature and low-cost fabrication process [2]. Optical parametric amplifications based on four-wave-mixing (FWM) in SOI waveguide have been theoretically investigated with the model of the coupled NLS equations describing the slowly varying amplitude of the optical waves [3–5]. The most commonly used numerical scheme for solving the NLSE is the split-step Fourier (SSF) method due to its simplicity for implementation and high computational efficiency [6–9]. Since phase-sensitive amplifiers (PSA) have the potential applications in optical communication, optical processing, photon detection, and optical spectroscopy and sensing [10], it is significant and crucial to model and investigate phase-sensitive amplification in SOI waveguide by using the coupled NLS equations describing power and phase of the optical waves for nonlinear photonic integration. The coupled NLS equations describing power and phase have been used to analyze the parametric process in fibers [11, 12]. Particularly,

Hansryd et al. used the coupled NLS equations to analyze fiber-based optical parametric amplifiers [11]. Compared with optical fibers, the silicon waveguide has some additional complications, such as two-photon absorption (TPA), free-carrier absorption (FCA), and free-carrier dispersion (FCD). Therefore, we should consider TPA, FCA, and FCD in silicon waveguide to develop the coupled NLS equations.

In this paper, through analyzing the coupled NLS equations describing slowly varying amplitude of the optical waves in FWM process, we develop the model of PS amplification based on coupled NLS equations describing power and phase of the optical waves in a width-modulated SOI channel waveguide. The model describes the power and phase variation in the silicon waveguide, which can be solved by the split-step Fourier and Runge-Kutta integration methods [5, 7–9, 13–15]. The calculation process using the solving methods has been discussed. The numerical results show that the coupled NLS equations can perfectly describe and character the PS amplification process in silicon waveguides.

2. Theory

The PS parametric amplification can be realized using FWM effect. Here, we focus on the degenerate FWM, which

typically involves two pump photons at frequency ω_p passing their energy to a signal wave at frequency ω_s and an idler wave at frequency ω_i as the relation $2\omega_p = \omega_s + \omega_i$ holds. The signal wave is amplified and the idler wave is generated during the FWM process. Moreover, the phase-matching among the interacting waves is required in the FWM process, which is achieved when the mismatch in the propagation constants of the pump, signal, and idler waves is compensated by the phase shift due to SPM and XPM, such that $\Delta k = \Delta\beta + 2\gamma_p P_{\text{pump}} = 0$. Here $\Delta\beta = k_s + k_i - 2k_p$ is the phase mismatch due to the linear dispersion, P_{pump} is the pump power, $\gamma_p = \omega_p n_2 / c A_{\text{eff}}$ is the nonlinear waveguide parameter, $n_2 = 12\pi^2 \chi^{(3)} / n_0 c$ is the nonlinear index coefficient, c is the speed of light, n_0 is the linear refractive index, and A_{eff} is the effective area of the propagating mode, respectively.

The pump and signal waves are identically polarized in the fundamental quasi-TM mode. To depict the nonlinear optical interaction of the pump, signal, and idler in the waveguide, we use the formalism described in [16–18] and take into account the effects of TPA, FCA, and FCD. The coupled NLS equations describing slowly varying amplitude of the different optical waves read as

$$\begin{aligned}
& \frac{\partial A_p}{\partial z} + \frac{i\beta_{2p}}{2} \frac{\partial^2 A_p}{\partial T^2} \\
&= -\frac{1}{2} (\alpha_p + \alpha_{fp}) A_p + i \left(\gamma_p + i \frac{\beta_{\text{TPA}}}{2A_{\text{eff}}} \right) |A_p|^2 A_p \\
&+ 2i \left(\gamma_p + i \frac{\beta_{\text{TPA}}}{2A_{\text{eff}}} \right) (|A_s|^2 + |A_i|^2) A_p \\
&+ i \frac{2\pi}{\lambda_p} \delta n_{fp} A_p + 2i\gamma_p A_s A_i A_p^* \exp(i\Delta\beta z), \\
& \frac{\partial A_s}{\partial z} + d_s \frac{\partial A_s}{\partial T} + \frac{i\beta_{2s}}{2} \frac{\partial^2 A_s}{\partial T^2} \\
&= -\frac{1}{2} (\alpha_s + \alpha_{fs}) A_s + i \left(\gamma_s + i \frac{\beta_{\text{TPA}}}{2A_{\text{eff}}} \right) |A_s|^2 A_s \\
&+ 2i \left(\gamma_s + i \frac{\beta_{\text{TPA}}}{2A_{\text{eff}}} \right) (|A_p|^2 + |A_i|^2) A_s \\
&+ i \frac{2\pi}{\lambda_s} \delta n_{fs} A_s + i\gamma_s A_p^2 A_i^* \exp(-i\Delta\beta z), \\
& \frac{\partial A_i}{\partial z} + d_i \frac{\partial A_i}{\partial T} + \frac{i\beta_{2i}}{2} \frac{\partial^2 A_i}{\partial T^2} \\
&= -\frac{1}{2} (\alpha_i + \alpha_{fi}) A_i + i \left(\gamma_i + i \frac{\beta_{\text{TPA}}}{2A_{\text{eff}}} \right) |A_i|^2 A_i \\
&+ 2i \left(\gamma_i + i \frac{\beta_{\text{TPA}}}{2A_{\text{eff}}} \right) (|A_p|^2 + |A_s|^2) A_i \\
&+ i \frac{2\pi}{\lambda_i} \delta n_{fi} A_i + i\gamma_i A_p^2 A_s^* \exp(-i\Delta\beta z),
\end{aligned} \tag{1}$$

where A_j is the slowly varying amplitude ($j = p, s, i$), z is the propagation distance, and β_{2j} is the GVD coefficient. Time

$T = t - z/v_{gp}$ is measured in a reference frame moving with pump pulse traveling at speed v_{gp} . The two walk-off parameters of the signal and idler are defined as $d_s = \beta_{1s} - \beta_{1p}$ and $d_i = \beta_{1i} - \beta_{1p}$, respectively, where β_{1j} is the inverse of the group velocity. The nonlinear coefficient $\gamma_j = \omega_j n_2 / c A_{\text{eff}}$ with $n_2 = 6 \times 10^{-18} \text{ m}^2 \text{ W}^{-1}$ and $\beta_{\text{TPA}} = 5 \times 10^{-12} \text{ m W}^{-1}$ is the coefficient of TPA at the wavelength of 1550 nm [2].

In (1), α_j accounts for the linear loss and $\alpha_{fj} = \sigma_j N_c$ represents FCA, where σ_j is the FCA coefficient and N_c is the free-carrier density generated by pump, signal, and idler pulses. $\delta n_{fj} = \zeta_j N_c$ is the free-carrier induced index change. These free-carrier parameters are obtained by solving [3, 19]

$$\begin{aligned}
\sigma_j &= 1.45 \times 10^{-21} \left(\frac{\lambda_j}{\lambda_{\text{ref}}} \right)^2 \text{ m}^2, \\
\zeta_j &= -1.35 \times 10^{-27} \left(\frac{\lambda_j}{\lambda_{\text{ref}}} \right)^2 \text{ m}^3,
\end{aligned} \tag{2}$$

$$\frac{\partial N_c(z, t)}{\partial t} = \frac{\pi\beta_{\text{TPA}}}{2h\omega_p A_{\text{eff}}} |A_p(z, t)|^4 - \frac{N_c(z, t)}{\tau_c},$$

where λ_j is the wavelength, $\lambda_{\text{ref}} = 1550 \text{ nm}$, h is Planck's constant, and $\tau_c \approx 1 \text{ ns}$ is the carrier lifetime. In order to describe the power and phase of the different waves, we should find the coupled NLS equations describing power and phase. Let $A_j = |A_j| \exp(i\varphi_j)$, $P_j = |A_j|^2$; (1) can be rewritten in terms of optical powers and phase:

$$\begin{aligned}
\frac{\partial P_p}{\partial z} &= \beta_{2p} \frac{\partial P_p}{\partial T} \frac{\partial \varphi_p}{\partial T} + \beta_{2p} P_p \frac{\partial^2 \varphi_p}{\partial T^2} - (\alpha_p + \alpha_{fp}) P_p \\
&- \frac{\beta_{\text{TPA}}}{A_{\text{eff}}} P_p^2 - \frac{2\beta_{\text{TPA}}}{A_{\text{eff}}} (P_s + P_i) P_p \\
&- 4\gamma_p (P_s P_i P_p^2)^{1/2} \sin \theta, \\
\frac{\partial P_s}{\partial z} &= -d_s \frac{\partial P_s}{\partial T} + \beta_{2s} \frac{\partial P_s}{\partial T} \frac{\partial \varphi_s}{\partial T} + \beta_{2s} P_s \frac{\partial^2 \varphi_s}{\partial T^2} - (\alpha_s + \alpha_{fs}) P_s \\
&- \frac{\beta_{\text{TPA}}}{A_{\text{eff}}} P_s^2 - \frac{2\beta_{\text{TPA}}}{A_{\text{eff}}} (P_p + P_i) P_s \\
&+ 2\gamma_s (P_s P_i P_p^2)^{1/2} \sin \theta, \\
\frac{\partial P_i}{\partial z} &= -d_i \frac{\partial P_i}{\partial T} + \beta_{2i} \frac{\partial P_i}{\partial T} \frac{\partial \varphi_i}{\partial T} + \beta_{2i} P_i \frac{\partial^2 \varphi_i}{\partial T^2} - (\alpha_i + \alpha_{fi}) P_i \\
&- \frac{\beta_{\text{TPA}}}{A_{\text{eff}}} P_i^2 - \frac{2\beta_{\text{TPA}}}{A_{\text{eff}}} (P_p + P_s) P_i \\
&+ 2\gamma_i (P_s P_i P_p^2)^{1/2} \sin \theta, \\
\frac{\partial \varphi_p}{\partial z} &= -\frac{\beta_{2p}}{2\sqrt{P_p}} \frac{\partial^2 \sqrt{P_p}}{\partial T^2} + \frac{\beta_{2p}}{2} \left(\frac{\partial \varphi_p}{\partial T} \right)^2 + \gamma_p P_p + \frac{2\pi}{\lambda_p} \delta n_{fp} \\
&+ 2\gamma_p (P_s + P_i) + 2\gamma_p (P_s P_i)^{1/2} \cos \theta,
\end{aligned}$$

$$\begin{aligned}
\frac{\partial \varphi_s}{\partial z} &= -d_s \frac{\partial \varphi_s}{\partial T} - \frac{\beta_{2s}}{2\sqrt{P_s}} \frac{\partial^2 \sqrt{P_s}}{\partial T^2} + \frac{\beta_{2s}}{2} \left(\frac{\partial \varphi_s}{\partial T} \right)^2 + \gamma_s P_s \\
&\quad + \frac{2\pi}{\lambda_s} \delta n_{fs} + 2\gamma_s (P_p + P_i) + \gamma_s \left(\frac{P_p P_i}{P_s} \right)^{1/2} \cos \theta, \\
\frac{\partial \varphi_i}{\partial z} &= -d_i \frac{\partial \varphi_i}{\partial T} - \frac{\beta_{2i}}{2\sqrt{P_i}} \frac{\partial^2 \sqrt{P_i}}{\partial T^2} + \frac{\beta_{2i}}{2} \left(\frac{\partial \varphi_i}{\partial T} \right)^2 + \gamma_i P_i + \frac{2\pi}{\lambda_i} \delta n_{fi} \\
&\quad + 2\gamma_i (P_p + P_s) + \gamma_i \left(\frac{P_p P_s}{P_i} \right)^{1/2} \cos \theta,
\end{aligned} \tag{3}$$

where $\theta = \Delta\beta z + \varphi_s + \varphi_i - 2\varphi_p$ is the relative phase and φ_p , φ_s , and φ_i are the phases of the pump, signal, and idler. Equations (3) can be solved by split-step Fourier and Runge-Kutta integration methods, which are discussed in the following part.

First, we assume the propagation length is divided into a large number of segments. Each segment length is defined as step length h , which is small enough that the nonlinear effects and dispersion can be treated independently. Two steps should be carried out for the propagation length from z to $z+h$. In the first step, the nonlinearity acts alone, and (3) are simplified as ordinary differential equations:

$$\begin{aligned}
\frac{dP_p}{dz} &= -(\alpha_p + \alpha_{fp}) P_p - \frac{\beta_{TPA}}{A_{\text{eff}}} P_p^2 \\
&\quad - \frac{2\beta_{TPA}}{A_{\text{eff}}} (P_s + P_i) P_p - 4\gamma_p (P_s P_i P_p^2)^{1/2} \sin \theta, \\
\frac{dP_s}{dz} &= -(\alpha_s + \alpha_{fs}) P_s - \frac{\beta_{TPA}}{A_{\text{eff}}} P_s^2 - \frac{2\beta_{TPA}}{A_{\text{eff}}} (P_p + P_i) P_s \\
&\quad + 2\gamma_s (P_s P_i P_p^2)^{1/2} \sin \theta, \\
\frac{dP_i}{dz} &= -(\alpha_i + \alpha_{fi}) P_i - \frac{\beta_{TPA}}{A_{\text{eff}}} P_i^2 - \frac{2\beta_{TPA}}{A_{\text{eff}}} (P_p + P_s) P_i \\
&\quad + 2\gamma_i (P_s P_i P_p^2)^{1/2} \sin \theta, \\
\frac{d\varphi_p}{dz} &= \gamma_p P_p + \frac{2\pi}{\lambda_p} \delta n_{fp} + 2\gamma_p (P_s + P_i) \\
&\quad + 2\gamma_p (P_s P_i)^{1/2} \cos \theta, \\
\frac{d\varphi_s}{dz} &= \gamma_s P_s + \frac{2\pi}{\lambda_s} \delta n_{fs} + 2\gamma_s (P_p + P_i) \\
&\quad + \gamma_s \left(\frac{P_p P_i}{P_s} \right)^{1/2} \cos \theta, \\
\frac{d\varphi_i}{dz} &= \gamma_i P_i + \frac{2\pi}{\lambda_i} \delta n_{fi} + 2\gamma_i (P_p + P_s) \\
&\quad + \gamma_i \left(\frac{P_p P_s}{P_i} \right)^{1/2} \cos \theta.
\end{aligned} \tag{4}$$

The above ordinary differential equations can be solved by Runge-Kutta method, and the results can be expressed as $P_p(z+h)'$, $P_s(z+h)'$, $P_i(z+h)'$, $\varphi_p(z+h)'$, $\varphi_s(z+h)'$, and $\varphi_i(z+h)'$, respectively. In the second step, dispersion acts alone mathematically,

$$\begin{aligned}
P_p(z+h) &= F_T^{-1} \left\{ F_T \left[P_p(z+h)' \exp(-2\beta_{2p}\omega^2 \varphi_p(z)h) \right] \right\}, \\
P_s(z+h) &= F_T^{-1} \left\{ F_T \left[P_s(z+h)' \exp(i\omega d_s h - 2\beta_{2s}\omega^2 \varphi_s(z)h) \right] \right\}, \\
P_i(z+h) &= F_T^{-1} \left\{ F_T \left[P_i(z+h)' \exp(i\omega d_i h - 2\beta_{2i}\omega^2 \varphi_i(z)h) \right] \right\}, \\
\varphi_p(z+h) &= F_T^{-1} \left\{ F_T \left[\varphi_p(z+h)' \exp\left(\frac{\omega^2 \beta_{2p}}{2\varphi_p(z)} h - \frac{\omega^2 \beta_{2p} \varphi_p(z)}{2} h \right) \right] \right\}, \\
\varphi_s(z+h) &= F_T^{-1} \left\{ F_T \left[\varphi_s(z+h)' \right. \right. \\
&\quad \left. \left. \times \exp\left(i\omega d_s h + \frac{\omega^2 \beta_{2s}}{2\varphi_s(z)} h - \frac{\omega^2 \beta_{2s} \varphi_s(z)}{2} h \right) \right] \right\}, \\
\varphi_i(z+h) &= F_T^{-1} \left\{ F_T \left[\varphi_i(z+h)' \right. \right. \\
&\quad \left. \left. \times \exp\left(i\omega d_i h + \frac{\omega^2 \beta_{2i}}{2\varphi_i(z)} h - \frac{\omega^2 \beta_{2i} \varphi_i(z)}{2} h \right) \right] \right\},
\end{aligned} \tag{5}$$

where F_T represents the Fourier-transform operation and ω is the frequency in the Fourier domain [18]. Therefore, the coupled NLS equations describing powers and phase of different optical waves are solved by split-step Fourier and Runge-Kutta integration methods. The detailed numerical results in the third part of the paper will show that the split-step Fourier and Runge-Kutta integration methods provide accurate and stable solution for the coupled NLS equations describing power and phase.

Here the coupled NLS equations describing power and phase are used to model and simulate the PS parametric amplification in a width-modulated SOI waveguide, which is comprised of three segments of channel waveguides with different widths and identical height as shown in Figure 1. Tapers are used to connect the three segments to avoid the mode mismatch induced by the variation of width [20]. In the first segment, the SOI waveguide with width of W_1 has an anomalous dispersion at the pump wavelength of 1550 nm, which acts as a PIA to amplify the signal and generate an

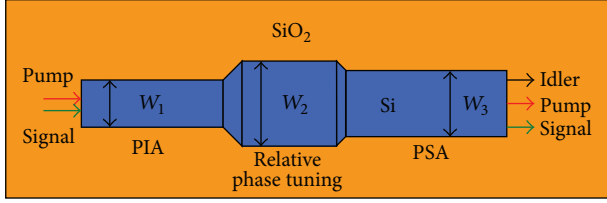


FIGURE 1: Illustration of the phase-sensitive parametric amplification in a width-modulated SOI channel waveguide with identical height.

idler. The relative phase at the output of the PIA is $\theta^{\text{Out-PIA}} = \Delta\beta_1 L_1 + \varphi_s(L_1) + \varphi_i(L_1) - 2\varphi_p(L_1)$, where $\Delta\beta_1$ is the linear phase mismatch of the silicon waveguide with width of W_1 and L_1 is the length of the first segment. The second segment is channel waveguide with width of W_2 , which has a normal dispersion at the pump wavelength. The relative phase at the input of the PSA is $\theta^{\text{In-PSA}} = \Delta\beta_1 L_1 + \Delta\beta_2 L_2 + \varphi_s(L_1 + L_2) + \varphi_i(L_1 + L_2) - 2\varphi_p(L_1 + L_2)$, where $\Delta\beta_2$ is the linear phase mismatch of the silicon waveguide with width of W_2 and L_2 is the length of the second segment. By changing the dispersion and length of the second segment, the relative phase $\theta^{\text{In-PSA}}$ can be set to an arbitrary value. The third silicon waveguide with width of W_3 acts as a PSA, which can amplify or deamplify the signal depending on the relative phase at the input of PSA $\theta^{\text{In-PSA}}$.

The widths W_1 , W_2 , and W_3 of the width-modulated SOI waveguide are assumed as 500 nm, 650 nm, and 580 nm, respectively, while the height is 800 nm. The linear propagation losses of the three segments are set to be 0.3 dB/cm, 0.2 dB/cm, and 0.25 dB/cm, respectively [21]. The PSA process is theoretically investigated with pump pulse of 20 ps at the wavelength of 1550 nm and continuous-wave signal at the wavelength of 1360 nm. According to the relation $2\omega_p = \omega_s + \omega_i$, the wavelength of the idler is 1801.7 nm. The dispersion parameters of our model are listed in Table 1.

3. Results and Discussion

The coupled NLS equations of (3) are solved by using split-step Fourier and Runge-Kutta integration methods to investigate the PS parametric amplification process in the width-modulated SOI channel waveguide as shown in Figure 2. The initial pump peak power is set to be 5 W, while the initial signal power is set to be 1 mW. From Figure 2(a), it is found that the relative phase θ quickly increases to $\pi/2$ when the initial phases of pump and idler are zero due to the generation of the idler and then decreases as the propagation length increases because of the large negative linear phase mismatch $\Delta\beta_1 = -1016 \text{ m}^{-1}$. It is clear that the signal peak power increases with the increase of the propagation length. That is because $\theta > 0$ along the propagation length, and the energy of the pump is transferred to signal and idler according to (3). It is expected that the signal peak power will decrease when further increasing the propagation length leads to $\theta < 0$, because the energy will be transferred back to pump. The output signal peak power is up to 5.07 mW, and relative phase

at the output of the PIA $\theta^{\text{Out-PIA}}$ is 0.127π when the length of the first segment is 8 mm. The second segment of the waveguide stops the decrease of the relative phase, because the positive linear phase mismatch of the second segment $\Delta\beta_2$ can compensate the negative linear phase mismatch of the first segment $\Delta\beta_1$. The relative phase is tuned to 0.63π and the signal peak power is increased to 7.57 mW through the second segment of the width-modulated waveguide as shown in Figure 2(b). The phase-sensitive amplification occurs in the third segment as shown in Figure 2(c). It exhibits exponential gain, and the signal peak power is amplified to 56.8 mW when the propagation length of the third segment is 10 mm. The relative phase in the third segment decreases as the propagation length increases due to a negative linear phase mismatch $\Delta\beta_3 = -389.5 \text{ m}^{-1}$. Therefore, the second segment of the width-modulated waveguide can tune the relative phase to an appropriate value to realize an effective PSA.

With the increase of the propagation length of the second segment, the relative phase increases from 0.127π to 2π as shown in Figure 3. However, the signal gain has a peak and a valley along the propagation length, which depends on the relative phase $\theta^{\text{In-PSA}}$. Here, we define the signal gain as the ratio of the output signal power to the input signal power for the width-modulated SOI waveguide. The maximum signal gain of 17.5 dB is obtained when $\theta^{\text{In-PSA}}$ is tuned to be 0.63π , while the minimal gain is 1.3 dB for $\theta^{\text{In-PSA}} = 1.64\pi$. From Figure 3, it is clear that the $\theta^{\text{In-PSA}}$ should be tuned between 0.127π and 0.98π for the PSA to obtain a gain larger than 15 dB, which means the length of the second segment should be less than 4.6 mm. From Figures 2 and 3, it is clear that the coupled NLS equations describing power and phase of the optical waves solved by split-step Fourier and Runge-Kutta integration methods provide an accurate description of the PS amplification process.

The linear phase mismatch $\Delta\beta$ is simulated for different waveguide widths as shown in Figure 4(a), which can be used to simulate the phase-sensitive amplification process for different width of the second segment. The relative phase and signal gain are investigated by tailoring the width W_2 of the second segment when the length of the second segment is 2 mm. The relative phase $\theta^{\text{In-PSA}}$ can be tuned from -0.11π to 0.95π by tailoring W_2 ranging from 500 nm to 700 nm as shown in Figure 4(b). It is found that the relative higher gain over 17 dB can be obtained for $0.41\pi < \theta^{\text{In-PSA}} < 0.7\pi$, which means that W_2 should be tailored to satisfy the condition: $610 \text{ nm} < W_2 < 660 \text{ nm}$.

4. Conclusion

The phase-sensitive parametric amplification process in a width-modulated silicon waveguide is described by the model of coupled NLS equations describing power and phase of the optical waves, which can be solved by the split-step Fourier and Runge-Kutta integration methods. Numerical results show that the split-step Fourier and Runge-Kutta integration methods provide accurate and stable solution for coupled NLS equations, which can perfectly describe the PS amplification process in silicon waveguides, and the

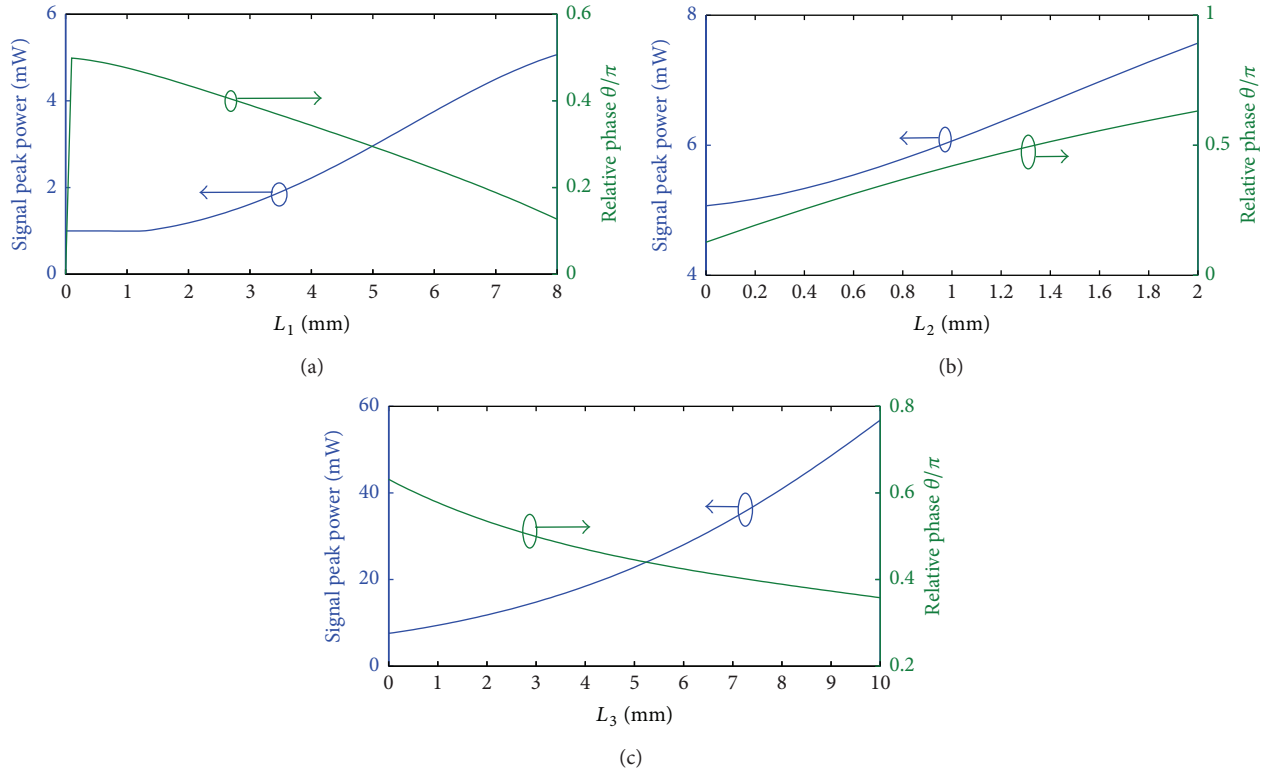


FIGURE 2: The signal peak power and relative phase as a function of the propagation length for the first segment (a), the second segment (b), and the third segment (c), respectively.

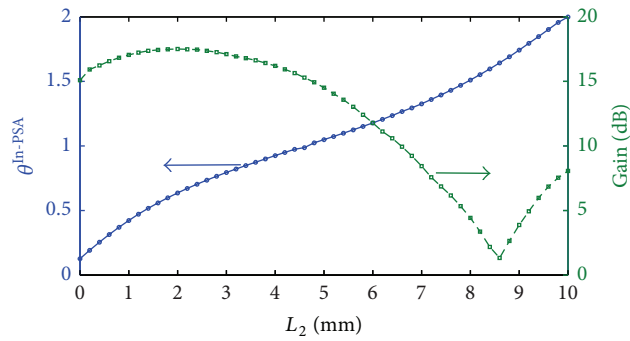


FIGURE 3: The relative phase at the input of PSA $\theta_{\text{In-PSA}}$ and signal gain as a function of the propagation length for the second segment.

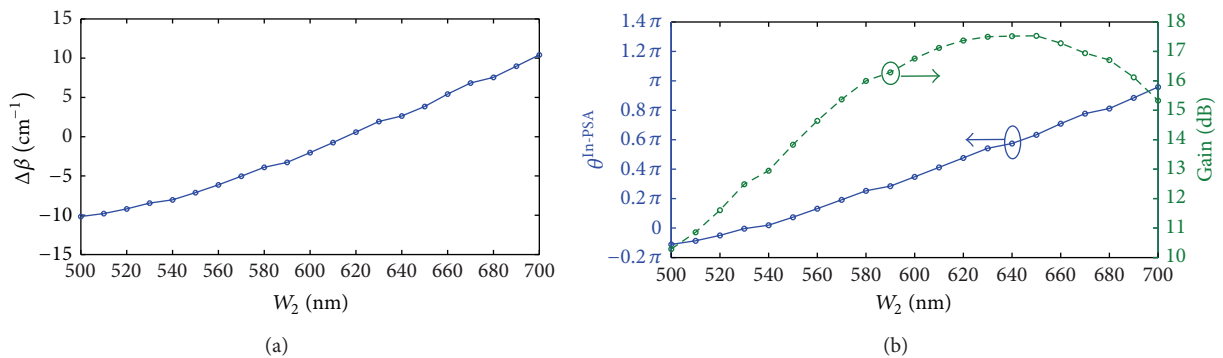


FIGURE 4: The linear phase mismatch $\Delta\beta$ (a), the relative phase at the input of PSA $\theta_{\text{In-PSA}}$ and signal gain (b) as a function of the waveguide width for the second segment.

TABLE 1

Width	$A_{\text{eff}} (\mu\text{m}^2)$	$\Delta\beta$ (1/m)	β_{1p} (ps/m)	β_{1s} (ps/m)	β_{1i} (ps/m)	β_{2p} (ps ² /m)	β_{2s} (ps ² /m)	β_{2i} (ps ² /m)
W_1	0.25	-1016	12912	12951	12972	-0.04603	0.5444	-0.7975
W_2	0.31	384.1	12791	12842	12850	0.004552	0.6014	-0.782
W_3	0.27	-389.5	12843	12891	12901	-0.02276	0.5749	-0.8014

PS amplification can be achieved in our designed width-modulated silicon waveguide.

Conflict of Interests

The authors declare that there is no conflict of interests regarding the publication of this paper.

Acknowledgment

This work was supported by the National Natural Science Foundation of China under Grant no. 61275134.

References

- [1] J. Leuthold, C. Koos, and W. Freude, "Nonlinear silicon photonics," *Nature Photonics*, vol. 4, no. 8, pp. 535–544, 2010.
- [2] L. Yin and G. P. Agrawal, "Impact of two-photon absorption on self-phase modulation in silicon waveguides," *Optics Letters*, vol. 32, no. 14, pp. 2031–2033, 2007.
- [3] Q. Lin, J. Zhang, P. M. Fauchet, and G. P. Agrawal, "Ultra-broadband parametric generation and wavelength conversion in silicon waveguides," *Optics Express*, vol. 14, no. 11, pp. 4786–4799, 2006.
- [4] Z. Wang, H. Liu, N. Huang, Q. Sun, and J. Wen, "Impact of dispersion profiles of silicon waveguides on optical parametric amplification in the femtosecond regime," *Optics Express*, vol. 19, no. 24, pp. 24730–24737, 2011.
- [5] X. Li, Z. Wang, and H. Liu, "Optimizing initial chirp for efficient femtosecond wavelength conversion in silicon waveguide by split-step Fourier method," *Applied Mathematics and Computation*, vol. 218, no. 24, pp. 11970–11975, 2012.
- [6] Q. Zhang and M. I. Hayee, "Symmetrized split-step fourier scheme to control global simulation accuracy in fiber-optic communication systems," *Journal of Lightwave Technology*, vol. 26, no. 2, pp. 302–316, 2008.
- [7] H. Wang, "Numerical studies on the split-step finite difference method for nonlinear Schrödinger equations," *Applied Mathematics and Computation*, vol. 170, no. 1, pp. 17–35, 2005.
- [8] X. Xu and T. Taha, "Parallel split-step Fourier methods for nonlinear Schrödinger-type equations," *Journal of Mathematical Modelling and Algorithms*, vol. 2, no. 3, pp. 185–201, 2003.
- [9] G. M. Muslu and H. A. Erbay, "Higher-order split-step Fourier schemes for the generalized nonlinear Schrödinger equation," *Mathematics and Computers in Simulation*, vol. 67, no. 6, pp. 581–595, 2005.
- [10] Z. Tong, C. Lundström, P. A. Andrekson, M. Karlsson, and A. Bogris, "Ultralow noise, broadband phase-sensitive optical amplifiers, and their applications," *IEEE Journal on Selected Topics in Quantum Electronics*, vol. 18, no. 2, pp. 1016–1032, 2012.
- [11] J. Hansryd, P. A. Andrekson, M. Westlund, J. Li, and P. Hedekvist, "Fiber-based optical parametric amplifiers and their applications," *IEEE Journal on Selected Topics in Quantum Electronics*, vol. 8, no. 3, pp. 506–520, 2002.
- [12] R. Hang, J. Lasri, P. S. Devgan, V. Grigoryan, P. Kumar, and M. Vasilyev, "Gain characteristics of a frequency nondegenerate phase-sensitive fiber-optic parametric amplifier with phase self-stabilized input," *Optics Express*, vol. 13, no. 26, pp. 10483–10493, 2005.
- [13] S. Zhang, Z. Deng, and W. Li, "A precise Runge-Kutta integration and its application for solving nonlinear dynamical systems," *Applied Mathematics and Computation*, vol. 184, no. 2, pp. 496–502, 2007.
- [14] M. Z. Liu, S. F. Ma, and Z. W. Yang, "Stability analysis of Runge-Kutta methods for unbounded retarded differential equations with piecewise continuous arguments," *Applied Mathematics and Computation*, vol. 191, no. 1, pp. 57–66, 2007.
- [15] B. S. Attili, K. Furati, and M. I. Syam, "An efficient implicit Runge-Kutta method for second order systems," *Applied Mathematics and Computation*, vol. 178, no. 2, pp. 229–238, 2006.
- [16] Z. Wang, H. Liu, N. Huang, Q. Sun, and J. Wen, "Influence of spectral broadening on femtosecond wavelength conversion based on four-wave mixing in silicon waveguides," *Applied Optics*, vol. 50, no. 28, pp. 5430–5436, 2011.
- [17] R. L. Espinola, J. I. Dadap, R. M. Osgood Jr., S. J. McNab, and Y. A. Vlasov, "C-band wavelength conversion in silicon photonic wire waveguides," *Optics Express*, vol. 13, no. 11, pp. 4341–4349, 2005.
- [18] G. P. Agrawal, *Nonlinear Fiber Optics*, 4th edition, 2007.
- [19] L. Yin, Q. Lin, and G. P. Agrawal, "Soliton fission and supercontinuum generation in silicon waveguides," *Optics Letters*, vol. 32, no. 4, pp. 391–393, 2007.
- [20] B. Jin, J. Yuan, C. Yu et al., "Efficient and broadband parametric wavelength conversion in a vertically etched silicon grating without dispersion engineering," *Optics Express*, vol. 22, pp. 6257–6268, 2014.
- [21] H. Rong, Y. Kuo, A. Liu, M. Paniccia, and O. Cohen, "High efficiency wavelength conversion of 10 Gb/s data in silicon waveguides," *Optics Express*, vol. 14, no. 3, pp. 1182–1188, 2006.